Available online at www.sciencedirect.com
SCIENCE DIRECT®
Bioorganic & Medicinal Chemistry 13 (2005) 5213–5217
Bioorganic & Medicinal Chemistry

Imaging amyloid β peptide oligomeric particles in solution

Jijun Dong, Robert P. Apkarian and David G. Lynn*

Center for the Analysis of SupraMolecular Self-assemblies, Integrated Microscopy and Microanalytical Facility, Departments of Chemistry and Biology, Emory University, 1521 Dickey Drive, Atlanta, GA 30322, USA

Received 16 April 2005; revised 22 May 2005; accepted 23 May 2005
Available online 29 June 2005

Abstract—While all protein misfolding diseases are characterized by fibrous amyloid deposits, the favorable free energy and strongly cooperative nature of the self-assembly have complicated the development of therapeutic strategies aimed at preventing their formation. As structural models for the amyloid fibrils approach atomic resolution, increasing evidence suggests that early folding intermediates, rather than the final structure, are more strongly associated with the loss of neuronal function. For that reason we now demonstrate the use of cryo-etch high-resolution scanning electron microscopy (cryo-HRSEM) for the direct observation of pathway intermediates in amyloid assembly. A congener of the Aβ peptide of Alzheimer's disease, Aβ(13–21), samples a variety of time-dependent self-assembles in a manner similar to those seen for larger proteins. A morphological description of these intermediates is the first step towards their structural characterization and the definition of their role in both amyloid assembly and neurotoxicity.

More than 20 widely different maladies, including Alzheimer's, Parkinson's, Huntington's, and human prion diseases, are recognized as protein conformational disorders.[1,2] Each is associated with a specific protein conformational rearrangement that promotes self-aggregation and the loss of cellular function.[3,4] Although the proteins identified in these diseases have very different primary sequences and biochemical roles, the aggregated forms, termed 'amyloid,' share many common characteristics such as being rich in pleated β-sheet structure, appearing on electron microscopy as non-branching fibrils with average diameters of 7–10 nm, binding specific histochemical dyes such as Congo Red, in this case, showing a unique 'apple-green' birefringence under crossed-polarized light, and resisting proteolysis and chemical solubilization.

Alzheimer's disease (AD), the most widely recognized of the conformational diseases, is a late-onset, progressive, and devastating neurodegenerative disorder characterized in individuals by loss of memory, task performance, and recognition of people and objects. AD now represents a major disease among aging populations, affecting approximately 25 million people worldwide, and the associated health care costs are growing rapidly. The characteristic pathology of AD patients is associated with extracellular neuritic plaque deposits as well as intracellular neurofibrillary tangles in brain tissues. The amyloid plaques are composed of aggregates of the β-amyloid peptide (Aβ), a 39–43 amino acid proteolytic fragment of a larger transmembrane protein termed amyloid precursor protein (APP). Although the pathological role of AP is unknown, this soluble peptide is present in all individuals at picomolar concentrations,[5,6] and the transition from soluble Aβ to the non-native conformation and aggregation into fibrils appears intimately associated with disease progression. Accordingly, efforts to understand the structural nature of amyloid fibrils, to elucidate the self-assembly pathway and the intermediates along the pathway, and to determine the factors affecting or participating in self-assembly could be crucial for therapeutic intervention.

The insoluble amyloid fibrils and deposits have long been thought to be the neurotoxic species.[7–9] However, increasing evidence now suggests a clear correlation between dementia and soluble Aβ oligomers.[10] Oligomeric species have appeared as common entities associated with fibril formation in various peptides, including Aβ, α-synuclein, polygutamine tracts and the larger prion proteins.[11–16] Moreover, antibodies specific for soluble oligomers, ones that do not bind monomers or fibrils but cross-react with very different oligomers, suggest

Keywords: Cryo-etch HESEM; Amyloid β peptide; Amyloid fibrils; Oligomeric particles; Intermediates; Self-assembly.
* Corresponding author. Tel.: +1 404 727 9348; fax: +1 404 727 6586; e-mail: dlynn2@emory.edu

0968-0896/$ - see front matter © 2005 Elsevier Ltd. All rights reserved.
doi:10.1016/j.bmc.2005.05.052

that these early assemblies have a common conformation distinct from the soluble monomers or fibrils.[17] The oligomers of Aβ, also referred as 'amyloid β derived diffusible ligands (ADDLs)', have been detected in vivo in both APP transgenic mice and in soluble extracts of AD patient brain tissues.[18–20] ADDLs, in the apparent absence of monomers and amyloid fibrils, specifically disrupt synaptic plasticity, leading presumably to early stage memory loss and subsequent long-term synapse degeneration and neuronal cell death.[21–25]

Several critical questions then emerge regarding these ADDLs. Since ADDLs can exist free of amyloid fibril for significant periods,[10–23] are they on- or off-pathway conformations that may or may not lead to amyloid formation? As the oligomers, certainly those formed by Aβ(1–42) either in vivo or in vitro, are heterodisperse, ranging from trimer to 24-mer,[10–20] could there be a critical size or a range of sizes that mediate the biological effects and/or initiate amyloid formation? Finally, and possibly most importantly, what are the structures of these various self-assembled ADDLs and what conditions favor the accumulation of those potential intermediates? These and related questions have resulted to our efforts to better characterize early assembly intermediates.

By dry/solution atomic force (AFM) and conventional transmission electron (TEM) microscopies, soluble oligomeric species generally appear in vitro as spherical particles 2.7–4.5 nm in diameter.[12,16,23,26,27] The presence and morphology of these particles are subject to differences in the analysis conditions. For example, amyloid β peptides display a number of surfactant-like properties, and even under real-time solution AFM, different surfaces can play a significant role in amyloid deposition.[11,19,28,29] Cryo-etch high-resolution scanning electron microscopy (cryo-etch HRSEM) of flash-frozen solutions was explored to evaluate directly the existence of oligomeric particles in solution independent of surface adsorption artifacts.

Cryo-etch HRSEM analyses are relatively new, never before having been applied to amyloid self-assembly, and accordingly we now report the development of experimental approaches suitable for such analyses. Although it is possible to perform such investigations with full-length Aβ(1–40/42), a shorter polypeptide based on residue 13–21 was chosen initially to improve sample solubility, increase the homogeneity of the preparations, and enhance experimental reproducibility. This central cassette of Aβ, ^{13}HHQALVFF^{21}A, maintains both a core sequence of the full-length peptide and the general hydrophilic N-/hydrophobic C-terminus, an amphiphilic patterning that appears important and critical for fibril formation.[28–33] This peptide also includes the Aβ(16–21) segment known to be crucial for fibril formation.[34–36] Indeed, the fibrils formed with this congener maintained the characteristic 10 nm diameter fibril structure and exhibited a characteristic red shift in the absorption spectrum of bound Congo Red, from 498 to 540 nm, indicating amyloid fibril structure.

Oligomeric particles of this Aβ(13–21) peptide were also observed early in the self-assembly process by AFM (Fig. 1). Spherical particles 2 ± 0.5 nm in diameter appeared at the earliest time points (Fig. 1A), by 72 h, 5 ± 0.5 nm particles and fibrils with 5 ± 0.5 or 10 ± 0.5 nm diameters coexist (Fig. 1B), and by 336 h, the particles are no longer present and only homogeneous long fibrils can be detected (Fig. 1C). Both oligomeric particles and mature fibrils were also detected by TEM (Fig. 2).

Particles with diameters 5 and 10 nm, as well as thin short filaments 5 nm in diameter, are labeled in Figure 2B as 1, 2, and 3 respectively. The 2 nm particles that appeared in AFM were not apparent in the TEM images—possibly the result of not absorbing to the TEM grids or not being stable to the high-voltage electron beam. Viewing these materials directly by cryo-etch HRSEM analyses offers an approach to overcome these limitations.

Different materials have different hydration properties and thus require different preparation and etching procedures. Accordingly, a series of cryo-etch experiments were performed to optimize the conditions. For Aβ(13–21), aliquots (5 μL) were taken at various time points from the self-assembling solution, introduced into flat-bottom-well gold planchets, and plunge-frozen in liquid ethane (−183 °C). Prior to analysis, planchets containing the frozen samples were stored in a slotted Teflon holder under liquid nitrogen (LN_2) in a double Dewar.

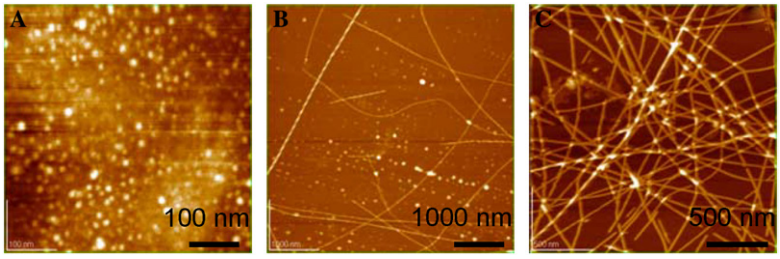

Figure 1. Self-assembly of Aβ peptide followed by AFM. One millimolar peptide was incubated in 25 mM MES buffer at pH 5.6 with 10 mM NaCl, at 24 h (A), 72 h (B), and 336 h (C). For AFM, 20 μL of the solution was placed on a clean silicon chip for 1 min, excess solution was removed with filter paper and the chip was rinsed with distilled H_2O. Tapping mode analysis on a JEOL JSPM-4210 employed ultra-sharp non-contact silicon cantilevers with typical frequencies between 240 and 350 kHz.

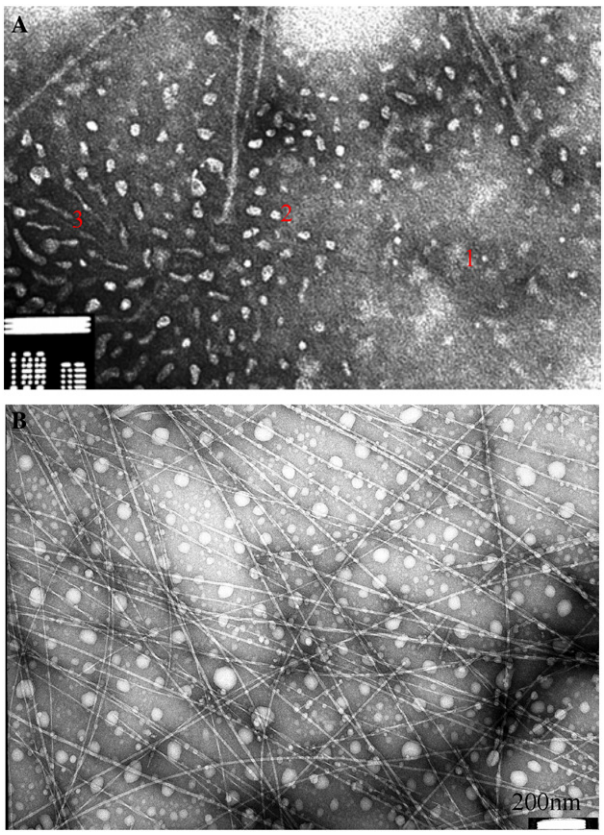

Figure 2. Self-assembly of Aβ peptide followed by TEM. One millimolar peptide was incubated in 25 mM MES buffer at pH 5.6 with 10 mM NaCl, imaged at 10 h (A) and after 2 weeks (B). For TEM sample preparation, 10 μL of the solution was placed on formvar/carbon 200 mesh grid for 1 min, excess solution was removed with filter paper and then stained with 1.5% uranyl acetate for 2 min.

For analysis, the samples were transferred to and mounted on the precooled (−170 °C) Gatan 3500 CT cryostage, fractured with a prechilled blade and washed with LN_2. Etching and coating of the fractured samples were carried out after transferring the cryostage to a Denton DV-602 chromium coater maintaining a vacuum of 2×10^{-7} Torr. The stage temperature was ramped from −170 to −105 °C to allow exposed ice to vaporize by sublimation (etching). Once complete, the temperature was returned to −170 °C and the sample was sputter-coated with chromium at a rate of 0.3 Å/s using a current of 50 mA at 300 V under a 5×10^{-3} Torr atmosphere of argon. The resulting 2-nm Cr film has the advantage of smaller grain sizes than previously reported metal coatings. Finally, the samples were removed from the coater and transferred to a DS-130F field emission scanning electron microscope (beam diameter ≈1 nm) fitted with dual cold finger anti-contamination traps and a Varian 860 cold-cathode gauge for monitoring the vacuum of the specimen. The cryo-stage was slowly ramped to −115 °C and allowed to equilibrate for 30 min. The microscope was operated at 25 kV.

Mature fibrils formed in 25 mM MES buffer pH 5.6 with 10 mM NaCl were investigated first to validate the technique (Figs. 3A and B). As shown in Figure 3B, granular ice appeared to obscure the amyloid assemblies. Amyloid fibril self-assembly solutions are commonly prepared in the presence of high buffer and NaCl concentrations as more representative of a biological matrix, however, our results, as well as those of other investigations,[37] show that frozen 2–3% saline gives granular icy 'fences' when etched. To avoid both high buffer concentrations and other ions that create salt-induced patterns, the peptides were directly dissolved in distilled deionized H_2O and the pH adjusted with NaOH. Higher peptide concentrations (3 mM) were required to obtain comparable assembly conditions, as confirmed by AFM analysis of their morphologies. Figures 3C–F shows a 72 h sample with fibrils and particles (D), and at higher magnification, clear smooth fibrils (E) and spherical particles (F). Significantly longer

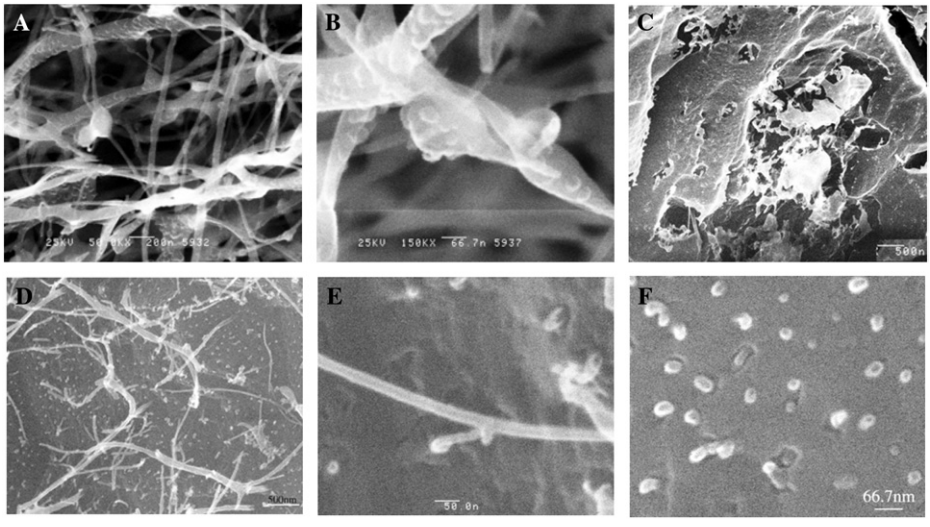

Figure 3. Cryo-etch high-resolution scanning electron microscopy (cryo-etch HRSEM) of Aβ peptide. (A and B) One millimolar peptide, dissolved in 25 mM MES buffer, pH 5.6 with 10 mM NaCl, was incubated at room temperature for 1 month and then imaged. (C–F) Three millimolar peptide was dissolved in distilled H_2O and pH was adjusted to 5.6 by slowly adding 1 M NaOH. After a 3-day incubation, samples were prepared for Cryo-etch HRSEM with a 18 min etching time at −105 °C. (C) Significant portion of the sample remained hydrated which can be seen at low and high magnification (C and D). Smooth fibrils were approximately 20 nm and spherical particles 10–20 nm in diameter (E and F).

etching times, 18 min at −105 °C, were required for the amyloids compared with the 1–5 min necessary for lipid surfactants.[38] A significant portion of the sample and a large number of fibrils remained hydrated even with 18 min etching times (Figs. 3C and D). The fibrils and particles in Figures 3E and F, with smooth surfaces suggesting bulk and loosely bound water had been removed, are still larger in size than seen in conventional TEM and AFM analyses, the fibrils being $\leqslant$20 nm in diameter and particles between 10 and 20 nm. We suspect the larger size remains the result of incomplete etching of tightly bound water. This appearance with the amyloid samples would be consistent with a high charge density at the surface of both particles and fibrils and heavily hydrated internal spacing as predicted most notably by the 'glycine vents' seen in computational modeling.[39,40] Further experiments to confirm these hypotheses with a wider range of amyloids and peptide assemblies are in progress.

Cryo-etch HRSEM of flash-frozen solutions nicely avoids the drying and surface artifacts present in AFM and TEM analyses. While sample freezing remains a variable that must be considered, these results suggest the convergence of these three imaging modalities allows for morphological and structural analysis of the rapidly forming amyloid assemblies. The ability to probe their lifetimes and distribution under different environmental conditions, in the presence of different metal ions,[41] and in the presence of molecular regulators offers unprecedented opportunity for defining assembly pathways and potential for developing small molecule probes of therapeutic importance for all conformational diseases.

Acknowledgment

We thank DOE ER15377 (D.G.L) for support and C. L. Emerson for AFM instrumentation.

References and notes

1. Kelly, J. W. *Curr. Opin. Struct. Biol.* **1998**, *8*, 101–106.
2. Carrell, R. W.; Lomas, D. A. *Lancet* **1997**, *350*, 134–138.
3. Ross, C. A.; Poirier, M. A. *Nat. Med.* **2004**, *10*(Suppl), S10–S17.
4. Carrell, R. W.; Gooptu, B. *Curr. Opin. Struct. Biol.* **1998**, *8*, 799–809.
5. Shoji, M.; Golde, T. E.; Ghiso, J.; Cheung, T. T.; Estus, S.; Shaffer, L. M.; Cai, X. D.; McKay, D. M.; Tintner, R.; Frangione, B., et al. *Science* **1992**, *258*, 126–129.
6. Seubert, P.; Vigo-Pelfrey, C.; Esch, F.; Lee, M.; Dovey, H.; Davis, D.; Sinha, S.; Schlossmacher, M.; Whaley, J.; Swindlehurst, C., et al. *Nature* **1992**, *359*, 325–327.
7. Lorenzo, A.; Yankner, B. A. *Proc. Natl. Acad. Sci. U.S.A.* **1994**, *91*, 12243–12247.
8. Pike, C. J.; Walencewicz, A. J.; Glabe, C. G.; Cotman, C. W. *Brain Res.* **1991**, *563*, 311–314.
9. Pike, C. J.; Walencewicz, A. J.; Glabe, C. G.; Cotman, C. W. *Eur. J. Pharmacol. Mol. Pharmacol. Sect.* **1991**, *207*, 367–368.
10. Klein, W. L. *Neurochem. Int.* **2002**, *41*, 345–352.
11. Kowalewski, T.; Holtzman, D. M. *Proc. Natl. Acad. Sci. U.S.A.* **1999**, *96*, 3688–3693.
12. Parbhu, A.; Lin, H.; Thimm, J.; Lai, R. *Peptides* **2002**, *23*, 1265–1270.
13. Serio, T. R.; Cashikar, A. G.; Kowal, A. S.; Sawicki, G. J.; Moslehi, J. J.; Serpell, L.; Arnsdorf, M. F.; Lindquist, S. L. *Science* **2000**, *289*, 1317–1321.
14. Poirier, M. A.; Li, H.; Macosko, J.; Cai, S.; Amzel, M.; Ross, C. A. *J. Biol. Chem.* **2002**, *277*, 41032–41037.
15. Kim, J.; Lee, M. *Biochem. Biophys. Res. Commun.* **2004**, *316*, 393–397.
16. Harper, J. D.; Wong, S. S.; Lieber, C. M.; Lansbury, P. T., Jr. *Biochemistry* **1999**, *38*, 8972–8980.
17. Kayed, R.; Head, E.; Thompson, J. L.; McIntire, T. M.; Milton, S. C.; Cotman, C. W.; Glabe, C. G. *Science* **2003**, *300*, 486–489.
18. Georganopoulou, D. G.; Chang, L.; Nam, J. M.; Thaxton, C. S.; Mufson, E. J.; Klein, W. L.; Mirkin, C. A. *Proc. Natl. Acad. Sci. U.S.A.* **2005**, *102*, 2273–2276.
19. Chang, L.; Bakhos, L.; Wang, Z.; Venton, D. L.; Klein, W. L. *J. Mol. Neurosci.* **2003**, *20*, 305–313.
20. Lambert, M. P.; Barlow, A. K.; Chromy, B. A.; Edwards, C.; Freed, R.; Liosatos, M.; Morgan, T. E.; Rozovsky, I.; Trommer, B.; Viola, K. L.; Wals, P.; Zhang, C.; Finch, C. E.; Krafft, G. A.; Klein, W. L. *Proc. Natl. Acad. Sci. U.S.A.* **1998**, *95*, 6448–6453.
21. Walsh, D. M.; Selkoe, D. *J. Protein Pept. Lett.* **2004**, *11*, 213–228.
22. Walsh, D. M.; Klyubin, I.; Fadeeva, J. V.; Rowan, M. J.; Selkoe, D. *J. Biochem. Soc. Trans.* **2002**, *30*, 552–557.
23. Lambert, M. P.; Viola, K. L.; Chromy, B. A.; Chang, L.; Morgan, T. E.; Yu, J.; Venton, D. L.; Krafft, G. A.; Finch, C. E.; Klein, W. L. *J. Neurochem.* **2001**, *79*, 595–605.
24. Walsh, D. M.; Klyubin, I.; Fadeeva, J. V.; Cullen, W. K.; Anwyl, R. ;.; Wolfe, M. S.; Rowan, M. J.; Selkoe, D. J. *Nature* **2002**, *416*, 535–539.
25. Kokubo, H.; Kayed, R.; Glabe, C. G.; Yamaguchi, H. *Brain Res.* **2005**, *1031*, 222–228.
26. Harper, J. D.; Wong, S. S.; Lieber, C. M.; Lansbury, P. T. *Chem. Biol.* **1997**, *4*, 119–125.
27. Stine, W. B.; Snyder, S. W.; Ladror, U. S.; Wade, W. S.; Miller, M. F.; Perun, T. J.; Holzman, T. F.; Krafft, G. A. *J. Protein Chem.* **1996**, *15*, 193–203.
28. Soreghan, B.; Kosmoski, J.; Glabe, C. *J. Biol. Chem.* **1994**, *269*, 28551–28554.
29. Gordon, D. J.; Balbach, J. J.; Tycko, R.; Meredith, S. C. *Biophys. J.* **2004**, *86*, 428–434.
30. Lu, K.; Jacob, J.; Thiyagarajan, P.; Conticello, V. P.; Lynn, D. G. *J. Am. Chem. Soc.* **2003**, *125*, 6391–6393.
31. Benzinger, T. L.; Gregory, D. M.; Burkoth, T. S.; Miller-Auer, H.; Lynn, D. G.; Botto, R. E.; Meredith, S. C. *Biochem.* **2000**, *39*, 3491–3499.
32. Burkoth, T. S.; Benzinger, T. L. S.; Urban, V.; Morgan, D. M.; Gregory, D. M.; Thiyagarajan, P.; Botto, R. E.; Meredith, S. C.; Lynn, D. G. *J. Am. Chem. Soc.* **2000**, *122*, 7883–7889.
33. Burkoth, T. S.; Benzinger, T. L. S.; Urban, V.; Lynn, D. G.; Meredith, S. C.; Thiyagarajan, P. *J. Am. Chem. Soc.* **1999**, *121*, 7429–7430.
34. Hilbich, C.; Kisters-Woike, B.; Reed, J.; Masters, C. L.; Beyreuther, K. *J. Mol. Biol.* **1992**, *228*, 460–473.
35. Hilbich, C.; Kisters-Woike, B.; Reed, J.; Masters, C. L.; Beyreuther, K. *J. Mol. Biol.* **1991**, *218*, 149–163.
36. Hughes, S. R.; Goyal, S.; Sun, J. E.; Gonzalez-DeWhitt, P.; Fortes, M. A.; Riedel, N. G.; Sahasrabudhe, S. R. *Proc. Natl. Acad. Sci. U.S.A.* **1996**, *93*, 2065–2070.
37. Menger, F. M.; Galloway, A. L.; Chlebowski, M. E.; Apkarian, R. P. *J. Am. Chem. Soc.* **2004**, *126*, 5987–5989.

38. Apkarian, R. P.; Wright, E. R.; Seredyuk, V. A.; Eustis, S.; Lyon, L. A.; Conticello, V. P.; Menger, F. M. *Microsc. Microanal.* **2003**, *9*, 286–295.
39. Morgan, D. M.; Lynn, D. G.; Lakdawala, A. S.; Snyder, J. P.; Liotta, D. C. *J. Chin. Chem. Soc. (Taipei Taiwan)* **2002**, *49*, 459–466.
40. Lakdawala, A. S.; Morgan, D. M.; Liotta, D. C.; Lynn, D. G.; Snyder, J. P. *J. Am. Chem. Soc.* **2002**, *124*, 15150–15151.
41. Morgan, D. M.; Dong, J.; Jacob, J.; Lu, K.; Apkarian, R. P.; Thiyagarajan, P.; Lynn, D. G. *J. Am. Chem. Soc.* **2002**, *124*, 12644–12645.